PHYSICAL REVIEW A VOLUME 20, NUMBER 5 NOVEMBER 1979

Total and partial cross sections for charge transfer in collisions of multicharged ions with atomic hydrogen

Hiroshi Ryufuku
Tokai Research Establishment, Japan Atomic Energy Research Institute, Tokai-mura, Naka-gun, Ibaraki 319-11, Japan

Tsutomu Watanabe*
Department of Applied Physics, Faculty of Engineering, The University of Tokyo, Bunkyo-ku, Tokyo 113, Japan
(Received 29 May 1979)

The total cross sections for charge transfer in $Ne^{10+} + H$, $Si^{14+} + H$, and $Ca^{20+} + H$ collisions are calculated for ion impact energies of 0.025–2000, 0.025–5000, and 0.1–10 keV/amu, respectively, by means of a unitarized-distorted-wave-approximation method. A scaling rule is derived from the results to predict cross section data. The partial cross sections for electron transfer into the individual orbitals around the projectiles are also investigated. The results show that the most probable principal quantum number of the final state is almost independent to impact energy below 100 keV/amu, while with increasing impact energy above 100 keV/amu it decreases considerably. The strong effects of level crossing and momentum transfer are confirmed to appear in the distributions of final-state population over angular momentum quantum number.

I. INTRODUCTION

Charge transfer processes involving heavy multicharged ions are one of the main subjects of recent theoretical and experimental investigations on ion-atom collisions from the viewpoint of pure academic interest as well as from that of practical applications to fusion research. Theoretical[1-10] and experimental[11-18] investigations on these processes have been reported by several workers. However, most of the experimental studies are concerned with the processes between partially stripped ions and atomic hydrogen.

Theoretical approaches which give results comparatively close to experimental values are the method of coupled molecular orbitals[2,7-9] for the low-energy region, a classical trajectory Monte Carlo method[3] for the intermediate-energy region, and a unitarized distorted-wave-approximation (UDWA) method[1,10] for the low-, intermediate-, and high-energy regions, where low energy denotes ion-impact energy below 10 keV/amu, intermediate energy that of 10–100 keV/amu, and high energy that above 100 keV/amu.

The primary UDWA work[1] (hereafter referred to as I) is applied to calculations of charge transfer cross sections for collisions of O^{8+}, He^{2+}, and H^+; results for O^{8+}, for example, showed excellent agreement with preliminary calculations of Salop and Olson[2] using the method of coupled molecular orbitals and the calculations of Olson and Salop[3] using the classical trajectory Monte Carlo method over the entire energy range considered by these authors. In the second UDWA work[10] (hereafter referred to as II), cross sections for charge transfer in collisions of Li^{3+}, Be^{4+}, B^{5+}, and O^{6+} ions with atomic hydrogen were calculated and the results compared with other theoretical results[2,3,7-9] and measured cross sections[11-18] for the collisions of completely and partially stripped ions having the same charge as those considered in the calculations. Comparisons showed that the UDWA method was very useful for impact energies 2–100 keV/amu but tended to overestimate the cross sections for impact energies greater than 100 keV/amu. In II, a scaling rule was also considered based on the UDWA cross sections and was applied to the experimental cross sections including the data obtained by Berkner *et al.*[19,20] for $Fe^{9+\sim25+} + H_2$ collision systems in which one-half the value of the measured cross sections were used. Plots of the scaled data almost fell along a single smooth curve in the intermediate- and high-energy regions.

In the present work, total and partial cross sections for charge transfer in collision of Ne^{10+}, Si^{14+}, and Ca^{20+} ions with atomic hydrogen are calculated. Furthermore, an attempt is made (a) to derive the scaling rule based on a theoretical basis including UDWA results for the highly ionized projectiles and (b) to examine the general properties of partial cross sections for charge transfer into the n, l, m orbitals around the projectiles, where n, l, and m denote the principal, angular, and magnetic quantum numbers, respectively.

In Sec. II a summary of the UDWA method is described; in Sec. III numerical results of the total cross sections are shown and the scaling rule is considered based on the results; and in Sec. IV partial cross sections with respect to the principal and angular quantum numbers, respec-

tively, are examined. Finally, in Sec. V a concluding summary of this paper is given. Atomic units are used throughout the paper, unless otherwise stated.

II. UDWA FORMULA

The details of the derivation of the UDWA formula have been described in II and only a summary will be presented here. We use a straight-line-trajectory impact-parameter approximation. The cross section for transition from the initial state $|0\rangle$ to the final state $|n\rangle$ is given by

$$\sigma_n = 2\pi \int_0^\infty P_n(\rho)\rho\, d\rho, \tag{2.1}$$

with

$$P_n(\rho) = |\langle n|S^{\rm int}|0\rangle|^2 \tag{2.2}$$

and

$$S^{\rm int} = T\exp\left(-i\int_{-\infty}^{\infty}\hat{H}^{\rm int}(t)\,dt\right), \tag{2.3}$$

where $P_n(\rho)$ is the transition probability for a given impact parameter ρ, $S^{\rm int}$ the S matrix in the interaction representation[21] and $\hat{H}^{\rm int}(t)$ the interaction matrix based on moving atomic orbitals for a given time t. The UDWA formula is obtained by an approximation in which the chronological-ordering operator T and all matrix elements except those involving the initial state $|0\rangle$ in the expansion series of Eq. (2.3) are ignored. Thus in the UDWA the matrix $S^{\rm int}$ is expressed as follows:

$$\langle 0|S^{\rm int}|0\rangle = \cos p^{1/2}, \tag{2.4}$$

$$\langle n|S^{\rm int}|0\rangle = -it_{n0}p^{1/2}\sin p^{1/2} \quad (n\neq 0), \tag{2.5}$$

with

$$p = \sum_{n=1}^{N}|t_{n0}|^2 \tag{2.6}$$

and

$$t_{n0} = \int_{-\infty}^{\infty}\langle n|\hat{H}^{\rm int}(t)|0\rangle\,dt, \tag{2.7}$$

where $|n\rangle$, $n=0, 1, 2, \ldots, N$ denotes all channels involved in the reaction.

Equation (2.7) is approximately equivalent to the semiclassical distorted-wave Born approximation (DWBA) formula[22] of the transition matrix elements; it is clear from Eqs. (2.4)–(2.6) that

$$\sum_{n=0}^{N}|\langle n|S^{\rm int}|0\rangle|^2 = 1, \tag{2.8}$$

that is, the unitarity of $S^{\rm int}$ is maintained in the approximate formula given by Eqs. (2.4)–(2.7), as this treatment is called the unitarized-distorted-wave approximation (UDWA).

In the calculations of charge transfer cross sections we introduce further approximation in which direct excitation and ionization channels are ignored.

III. TOTAL CROSS SECTION

In papers I and II, total cross sections for charge transfer in collisions of H^+, He^{2+}, Li^{3+}, Be^{4+}, B^{5+}, C^{6+}, and O^{8+} ions with atomic hydrogen have been reported. In the present paper, the charge transfer processes in collisions of Ne^{10+}, Si^{14+}, and Ca^{20+} ions with atomic hydrogen are considered; then, using the cross sections obtained, the scaling rule of total cross sections for ionic charge of the projectiles is established.

The calculations of the total cross sections were carried out according to the procedure described in II, as follows: The numerical calculation of the DWBA probabilities for charge transfer to all states having principal quantum number n was carried out for n up to $n_{\rm max}$, shown in Table I. For $n > n_{\rm max}$, it was estimated by extrapolation. Relative increases in the cross sections due to extrapolation are shown in Table II.

Total charge transfer cross sections calculated are shown in Table III, and only those for Ne^{10+}- and Si^{14+}-impact cases are also shown in Figs. 1 and 2. In the figures, experimental results obtained by Gardner *et al.*,[15] Meyer *et al.*,[17] and Berkner *et al.*[19] for impacts of projectiles having the same ionic charge are also shown for compar-

TABLE I. Values of $n_{\rm max}$ for $Ne^{10+}+H$, $Si^{14+}+H$, and $Ca^{20+}+H$ collisions.

Impact energy (keV/amu)	Ne^{10+}	Si^{14+}	Ca^{20+}
5000		4	
2000	6	12	
1000	8	12	
500	10	12	
200	10	12	
100	10	12	
50	10	10	
25	9	10	
10	8	8	11
5	6	8	
2.5	6	8	
1	6	8	11
0.5	6	8	
0.25	6	8	
0.1	6	8	11
0.05	6	8	
0.025	6	8	

TABLE II. Relative increase in the cross sections due to the extrapolation for $Ne^{10+}+H$, $Si^{14+}+H$, and $Ca^{20+}+H$ collisions.

Impact energy (keV/amu)	Ne^{10+}	Si^{14+}	Ca^{20+}
5000		3.41(−1) [a]	
2000	2.63(−1)	2.06(−1)	
1000	2.55(−1)	2.20(−1)	
500	2.68(−1)	3.29(−1)	
200	3.59(−1)	4.15(−1)	
100	3.24(−1)	3.16(−1)	
50	1.26(−1)	2.74(−1)	
25	1.98(−2)	4.94(−2)	
10	8.48(−4)		6.11(−3)

[a] 3.41(−1) means 3.41×10^{-1}.

ison. As is known from the other systems described in I and II, present results are larger than the experimental ones. From the property of the UDWA formula, it can be easily understood that UDWA results are a little overestimated for impact energy greater than about 100 keV/amu owing to the approximation in which the direct excitation and ionization channels are ignored.

We now consider the scaling of the cross sections with respect to ionic charge z. As described in II, it gives useful results to scale the impact energies as well as the cross sections as follows:

$$\sigma=\alpha\tilde{\sigma}(\tilde{E}) \tag{3.1}$$

and

TABLE III. UDWA cross sections for charge transfer in $Ne^{10+}+H$, $Si^{14+}+H$, and $Ca^{20+}+H$ collisions.

Impact energy (keV/amu)	Ne^{10+}	Si^{14+}	Ca^{20+}
5000		1.88(−21) [a]	
2000	5.03(−20)	1.50(−19)	
1000	1.24(−18)	3.45(−18)	
500	2.60(−17)	7.09(−17)	
200	6.41(−16)	1.46(−15)	
100	2.85(−15)	4.85(−15)	
50	5.00(−15)	7.96(−15)	
25	5.80(−15)	7.97(−15)	
10	5.96(−15)	6.82(−15)	9.30(−15)
5	5.39(−15)	7.17(−15)	
2.5	5.86(−15)	8.06(−15)	
1	7.21(−15)	8.80(−15)	1.22(−14)
0.5	7.45(−15)	9.33(−15)	
0.25	7.16(−15)	1.01(−14)	
0.1	5.47(−15)	1.02(−14)	1.37(−14)
0.05	4.93(−15)	9.64(−15)	
0.025	3.53(−15)	8.53(−15)	

[a] 1.88(−21) means 1.88×10^{-21} cm^2.

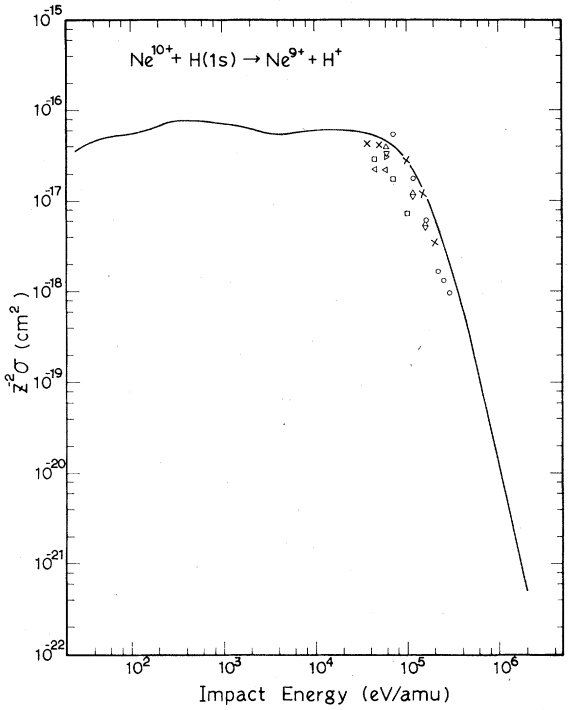

FIG. 1. Cross sections for the charge transfer process, $Ne^{10+}+H(1s)\rightarrow Ne^{9+}+H^+$, vs Ne^{10+} impact energy with $Z=10$. —indicates present results, × the results of Olson and Salop, Ref. 3 (classical trajectory Monte Carlo method). For comparison, also shown are the experimental cross sections for electron capture from atomic hydrogen by partially stripped ions: ○ (Fe^{10+}) Gardner *et al.* (Ref. 15); and ▽ (Fe^{10+}), △ (Mo^{10+}), ▷ (Au^{10+}), ◁ (W^{10+}), and □ (Ta^{10+}) Meyer *et al.* (Ref. 17).

$$E=\beta\tilde{E}\,, \tag{3.2}$$

where α and β are the scaling factors, $\tilde{\sigma}$ the scaled cross section, and $\tilde{E}$ the scaled impact energy.

Using the UDWA cross sections reported in I, II, and this paper, and iterating trial and error, the scaling factors are determined to be

$$\alpha=Z^{1.07} \tag{3.3}$$

and

$$\beta=Z^{0.464}\,. \tag{3.4}$$

The scaling factors given by Eqs. (3.3) and (3.4) are close to $\alpha'=Z$ and $\beta'=Z^{1/2}$. However, these α' and β' are not proper for the purpose of more precise scaling. Equations (3.3) and (3.4) will be discussed in connection with the distributions of final-state population in Sec. IV.

The scaled UDWA cross sections versus scaled energy are shown in Fig. 3 with the data obtained by Crandell *et al.*,[18] Meyer *et al.*,[17] Nutt *et al.*,[23] Gardner *et al.*,[15] and Berkner *et al.*[19,20] For

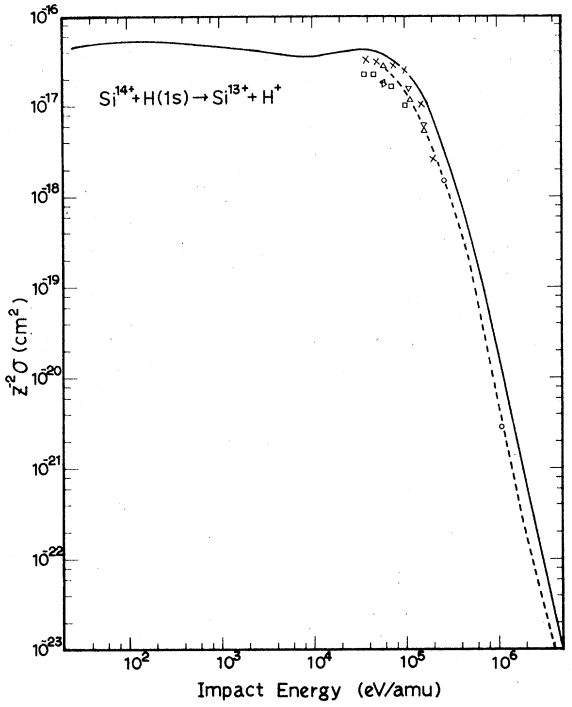

FIG. 2. Cross sections for the charge transfer process, $Si^{14+}+H(1s)\rightarrow Si^{13+}+H^+$, vs Si^{14+} impact energy with $Z=14$. — indicates present results, × the results of Olson and Salop, Ref. 3 (classical trajectory Monte Carlo method), and --- the results of the preliminary calculation with excitation and ionization channels. For comparison, also shown are the experimental cross sections for electron capture from atomic and molecular hydrogen by partially stripped ions: ▽ ($Fe^{14+}+H$), △ ($Mo^{14+}+H$), □ ($Ta^{14+}+H$), ▷ ($Au^{14+}+H$), and ◁ ($W^{14+}+H$) Meyer *et al.* (Ref. 17) and ○ ($Fe^{14+}+H_2$) Berkner *et al.* (Ref. 19), where the data for molecular hydrogen targets indicate one-half the value of the measured cross sections.

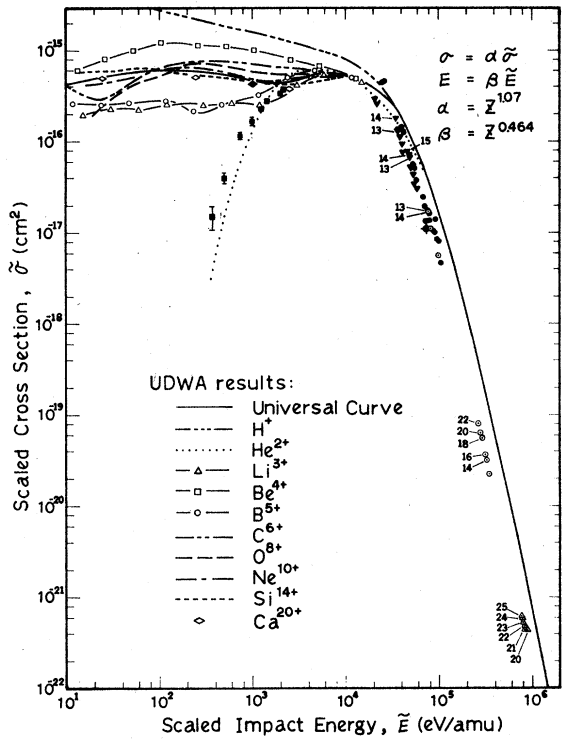

FIG. 3. Scaled cross sections $\tilde{\sigma}$ vs scaled impact energy $\tilde{E}$. The charge transfer cross sections and impact energy are expressed as $\sigma(E)=\alpha\tilde{\sigma}(\tilde{E})$ and $E=\beta\tilde{E}$, respectively, with $\alpha=Z^{1.07}$ and $\beta=Z^{0.464}$. The universal curve indicates the best-fitted curve to all UDWA results for $\tilde{E}>40$ keV/amu, to those except the H^+ results for $\tilde{E}=2$–40 keV/amu, and to Ne^{10+} and Si^{14+} results for $\tilde{E}<2$ keV/amu. Also shown are scaled experimental results: ▮ ($He^{2+}+H$) Nutt *et al.* (Ref. 23); ✦ ($O^{8+}+H$) Meyer *et al.* (Ref. 17); ◂▸ ($Ar^{8+}+H$) Crandall *et al.* (Ref. 18); ● ($Fe^{9+\sim13+}+H$) Gardner *et al.* (Ref. 15); ▼ ($Fe^{9+\sim15+}+H$) Meyer *et al.* (Ref. 17); ⊙ ($Fe^{9+\sim22+}+H_2$) Berkner *et al.* (Ref. 19), and △ ($Fe^{20+\sim25+}+H_2$) Berkner *et al.* (Ref. 20), where the numbers indicated express the value of ionic charge and the data for molecular hydrogen targets indicate one-half the value of the measured cross sections.

$\tilde{E}>8\times10^4$ eV/amu, the UDWA results fall along a single smooth "universal curve." With decreasing energy the deviations of the UDWA results become larger, where the cross sections are determined due to the level crossings. For $\tilde{E}<2\times10^3$ eV/amu, the universal curve is drawn as the scaled cross sections for Ne^{10+}, Si^{14+}, and Ca^{20+} impacts have minimum deviations. The UDWA results for high values of Z are expected to tend to the universal curve.

At low energies, $E\leq10$ keV/amu, molecular effects are certainly important. These effects are not rigorously included in the present method, that is, the final-state interactions are not included in the UDWA method. Therefore, the accuracy of the cross sections is theoretically obscure. However, the low-energy UDWA results are in as good agreement with available experimental data as molecular calculations.[10,18] We will examine the source of this problem below.

At low energies, the DWBA probability amplitude for charge transfer given by Eq. (2.38) of II results mainly from the points on the straight-line integration path $Z=vt$ where the argument of the exponential function vanishes; that is,

$$\omega_n^B+u_{nn}^{BB}=\omega_0^A+u_{00}^{AA} \tag{3.5}$$

is satisfied in Eq. (2.38) of II. The right-hand side of Eq. (3.5) means the energy level of the initial state perturbed by the potential due to the incident ion and the left-hand side means the energy level of the final state perturbed by the

potential due to the target nucleus. Accordingly, Eq. (3.5) denotes crossing of the energy levels of the two diabatic states. For example, the DWBA charge transfer probability $p(\rho)$ for O^{8+} + H(1s) collision at low energies $E \leq 1$ keV/amu denotes maxima at impact parameters of $\rho = 2.2$, 4.7, and 9.0 a.u. as shown in Figs. 4 and 5 of I. These values of the impact parameter correspond to the crossing points of the energy levels of O^{8+} + H(1s) and $O^{7+}(n = 3, 4, 5) + H^+$ systems, where n denotes the principal quantum number. One of the ambiguities of the UDWA cross section at low energies comes from the neglect of electron transfer from $O^{7+}(n = 5) + H^+$ to $O^{8+} + H(n = 2)$ diabatic states through the crossing point $R = 6.1$ a.u., where R denotes the internuclear distance. Therefore, this process is effective for an impact parameter smaller than $\rho_A = 6.1$. The error due to the neglect of this process can be estimated using a classical treatment to evaluate cross sections as the ratio of the area of radius ρ_A to that of radius $\rho = 9.0$ which corresponds to the most distant effective crossing point; that is, little charge transfer takes place for $\rho > 9.0$. Thus we obtain $\frac{1}{2} \times 6.1^2/9.0^2 \simeq 0.2$ as the relative error included in the UDWA cross section, where the probability for transition to the $O^{8+} + H(n = 2)$ diabatic state is assumed to be $\frac{1}{2}$.

Another error arises, at low energies, due to the approximation where the chronological-ordering operator T is neglected. As seen in Fig. 11 of I, at impact energies greater than 0.25 keV/amu, this approximation produces a relative error smaller than about 30% in the charge transfer probability.

After all, at energies $E \simeq 0.3$–10 keV/amu the relative error included in the UDWA cross sections is estimated to be, at most, about 50%.

At high energies $E \geq 100$ keV/amu, the errors described above are vanishingly small, and an additional error arises due to the approximation in which excitation and ionization channels are ignored. Although the inclusion of the excitation and ionization channels needs detailed examination of the selection of channel-state vectors, a preliminary calculation described below will be useful to estimate the error included in the present UDWA cross section. As an example, for the Si^{14+} + H(1s) collision the preliminary calculation was attempted using Eqs. (2.28) and (2.29) of II, where Coulomb wave functions centered on the proton were used for the continuum states and the post-collision perturbations due to the Coulomb force of the Si^{14+} ion were ignored. The results obtained are shown in Fig. 2 by the dashed line. At $E \simeq 1000$–2000 keV/amu, the estimated value with excitation and ionization channels denotes the maximum relative deviation from the original value without those channels, where the former is about 1/3.5 of the latter.

IV. PARTIAL CROSS SECTION

In this section we will examine partial cross sections for electron capture into the individual quantum states at intermediate and high energies $E \geq 10$ keV/amu. Although at high energies $E \geq 100$ keV/amu the UDWA cross sections are overestimated due to the neglect of ionization and excitation channels as described in Sec. III, the UDWA results will give useful information on the relative distributions of final-state population, since no other calculations have been reported.

We will also examine low-energy partial cross sections to know the trend of the UDWA results at low energies $E \leq 10$ keV/amu, while the UDWA gives inaccurate results due to the neglect of the final-state interactions and the chronological-ordering operator.

The partial cross section for electron transfer from the 1s state of a hydrogen atom to the nlm state of a fully stripped ion will be denoted by σ_{nlm}, where n, l, and m are the principal, orbital-angular, and magnetic quantum numbers, respectively. The n, l-dependent cross section σ_{nl} is defined by the sum of σ_{nlm} over m and the n-dependent cross section σ_n is defined by the sum of σ_{nl} over l, where the axis of quantization is taken to be in the impact direction.

To investigate the general properties of partial cross sections for charge transfer, we will examine the collisions of Ne^{10+} and Si^{14+} with H(1s) as examples. The n-dependent cross sections are shown in Fig. 4 with impact energy as a parameter. It is seen from the figure that, for both cases, the principal quantum number n_m of the most probable state indicates a maximum and the distribution over n is broadest at 100 keV/amu. With increasing energy, n_m decreases and the distribution becomes more and more narrow. This is considered to be due to the momentum-transfer effect; that is, with increasing energy the charge transfer probability indicates a maximum at the impact parameter being more and more small and, consequently, the electron transfer into the inner shell is more and more dominant. At low energies, charge transfer occurs through level crossing as described in Sec. III, and the distribution for $n > n_m$ becomes vanishingly small.

It is interesting to examine the "interpolated distributions" of final-state population over n obtained by interpolating the plotted points of σ_n vs n with a smooth curve. Figure 5 shows the depen-

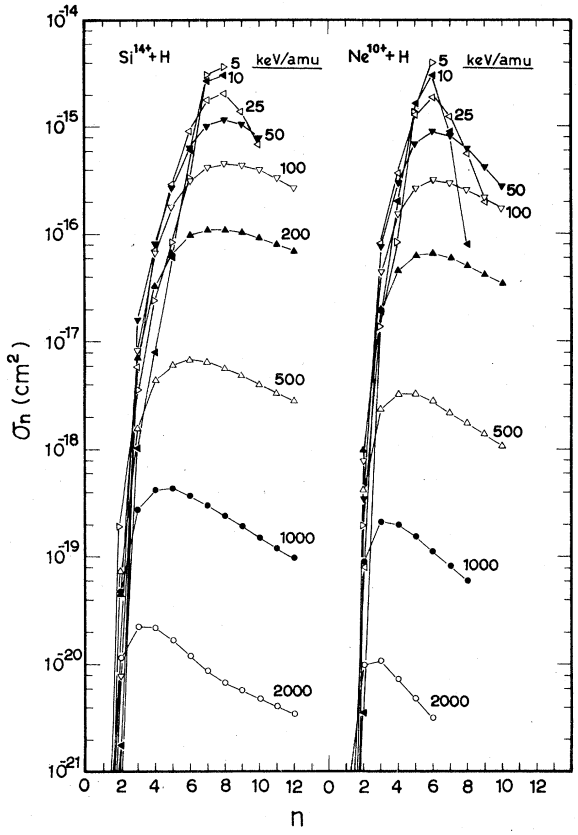

FIG. 4. Dependence of the partial cross sections σ_n for charge transfer in the $Ne^{10+}+H(1s)$ and $Si^{14+}+H(1s)$ collision systems on the principal quantum number n of the final state, for collision energies 5–2000 keV/amu.

dence of the interpolated principal quantum number, n_p at which the interpolated distributions indicate a maximum on ion-impact energy for the charge value of impacted ions being 2–14. We now consider the scaling factor β introduced in Sec. III. It is reasonably determined as the Z dependence of the fictitious-state energy corresponding to the principal quantum number n_p, since the dependence of the total cross sections on impact energy is uniformly determined by the relation of the impact energy to the most-probable-state energy, except in the low-impact-energy region. Thus

$$\beta \propto (Z/n_p)^2 . \tag{4.1}$$

Accordingly,

$$n_p \propto Z/\beta^{1/2} = Z^{0.768} . \tag{4.2}$$

Figure 6 shows the validity of Eq. (4.2) for $n=6$–14. Thus the theoretical meaning of β has been clarified.

In Fig. 7 the l-dependent cross sections for $Ne^{10+}+H$ collisions are shown with the principal quantum number of the final state as a parameter, at impact energies of 1, 25, and 500 keV/amu, which correspond to low, intermediate, and high energies, respectively. The l-dependent cross sections for 1 keV/amu indicates a maximum at $l<n-1$. In low-energy collisions, as stated before, the electron transfer occurs through level crossing. Therefore, the electron is mostly transferred into a state that has a wave function indicating a large amplitude at the crossing point, which usually has a smaller value of l than $n-1$. Thus the l-dependent cross sections for 1 keV/amu can be understood.

In the case of 25 keV/amu, the results for $n=3$ ~6 indicate a maximum at $l<n-1$ and those for $n \geq 7$ indicate a maximum at $l=n-1$. These results show that at intermediate energy the level crossing is still effective for the low-n states, but not for the high-n states. At the higher energy, the lower-n state becomes free from level-crossing effects. At further higher energies, as shown for the case of 500 keV/amu, momentum transfer becomes effective and the distributions in the higher value of l are suppressed considerably.

The partial cross sections σ_{nlm} are shown in Figs. 8–10, also for $Ne^{10+}+H$ collisions, at impact energies of 1, 25, and 500 keV/amu, where the quantization axis is taken along the direction

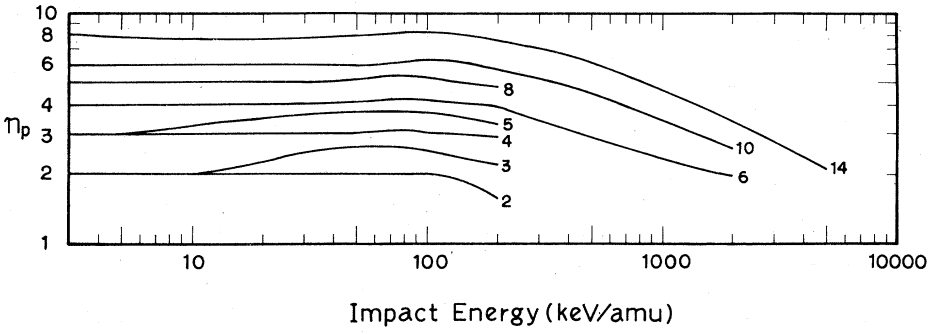

FIG. 5. Dependence of n_p on impact energy for the charge-value of impacted ions being 2–14, where n_p is the interpolated principal quantum number, at which the interpolated distributions of final state population over n indicate a maximum, where n is the principal quantum number of the orbitals around the projectiles.

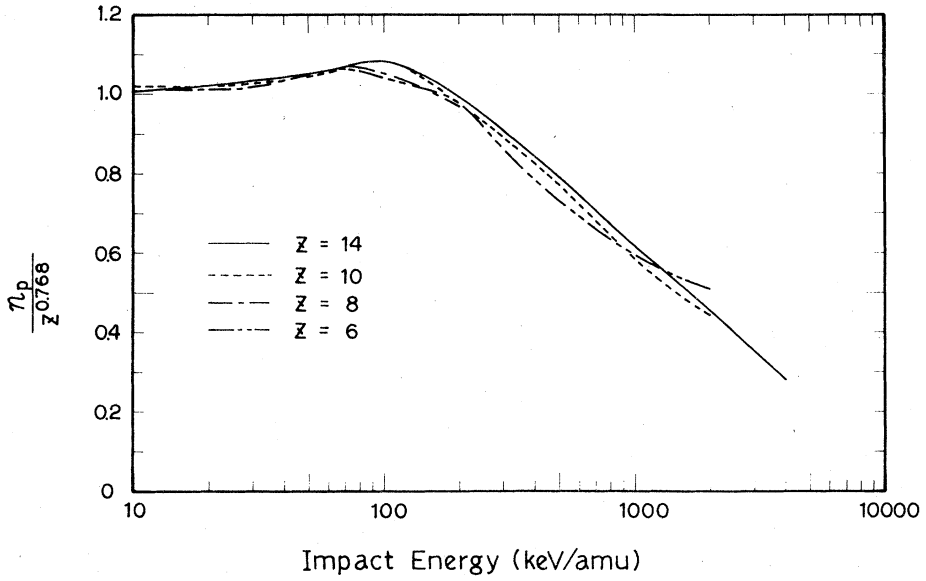

FIG. 6. Scaled n_p vs ion-impact energy.

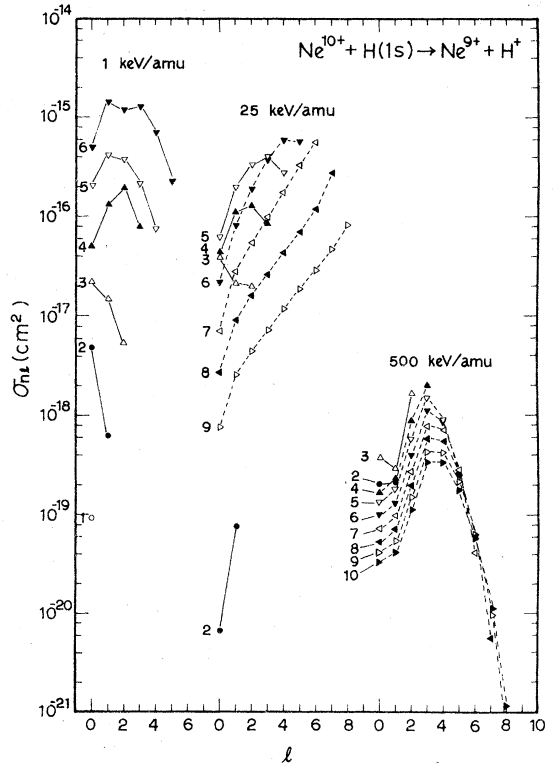

FIG. 7. Dependence of the partial cross sections σ_{nl} for charge transfer in the $Ne^{10+} + H(1s)$ collision system on the angular quantum number l of the final state, at collision energies of 1, 25, and 500 keV/amu, where the numbers indicated express the principal quantum number n.

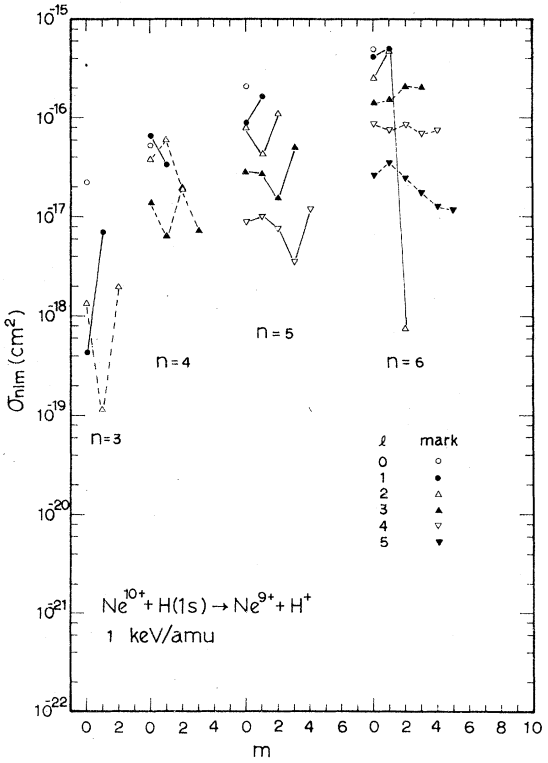

FIG. 8. Dependence of the partial cross sections σ_{nlm} for charge transfer in the $Ne^{10+} + H(1s)$ collision system on the magnetic quantum number m of the final state, with n and l as parameters, at the collision energy of 1 keV/amu.

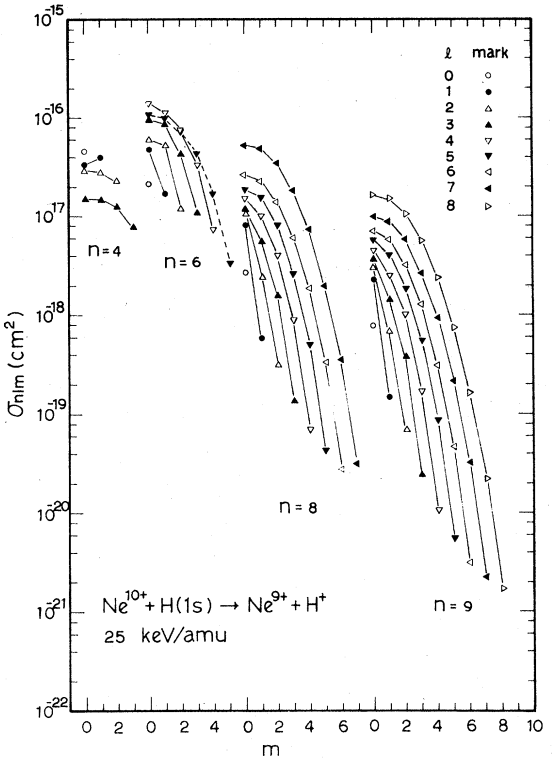

FIG. 9. Same as Fig. 8 for collision energy of 25 keV/amu.

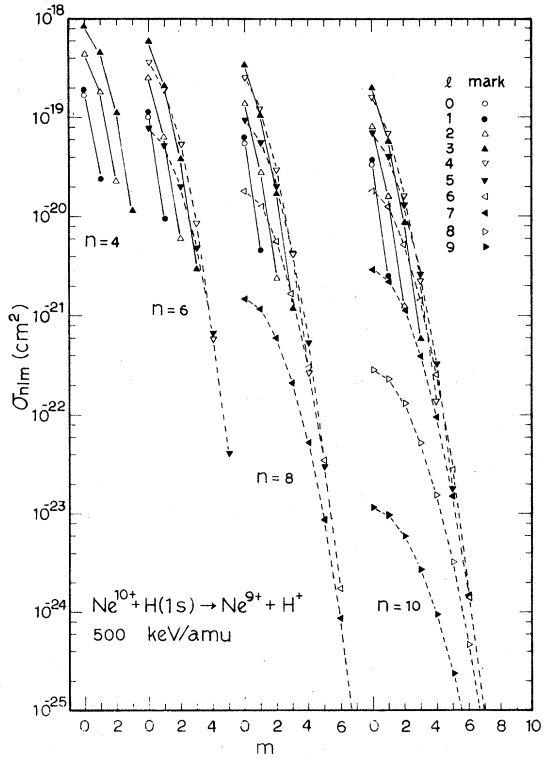

FIG. 10. Same as Fig. 9 for collision energy of 500 keV/amu.

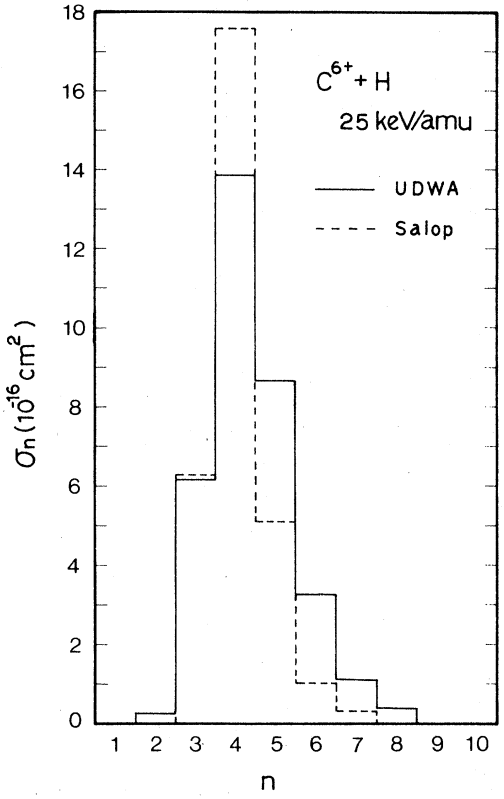

FIG. 11. Comparison of partial cross sections σ_n of the present work with that of Salop (Ref. 24) for charge transfer in the $C^{6+}+H(1s)$ collision system at a collision energy of 25 keV/amu.

of the movement of the impacted ion. It is seen from these figures that at lower energy the distributions over m are rather broad and with increasing impact energy the distributions become

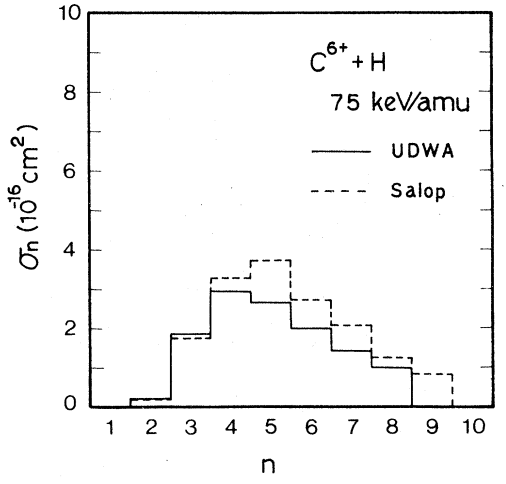

FIG. 12. Same as Fig. 11 for a collision energy of 75 keV/amu.

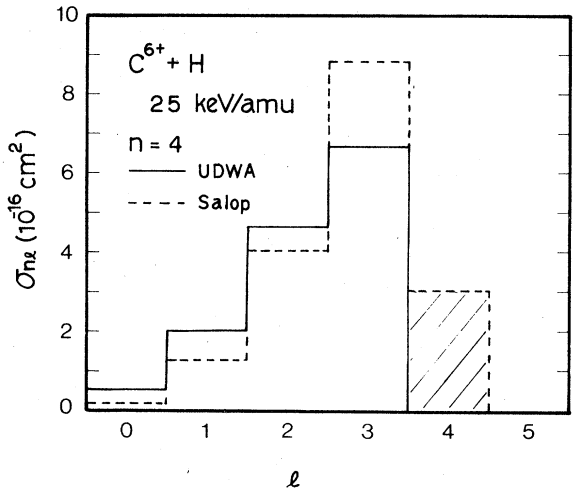

FIG. 13. Comparison of the partial cross sections σ_{nl} of the present work with that of Salop (Ref. 24) for the C^{6+} + H(1s) collision system at the collision energy of 25 keV/amu, where $n = 4$.

narrow, indicating a maximum at $m = 0$. The high probabilities of electron transfer into $m = 0$ states correspond to the classical picture that the electron is mostly captured into the orbitals on the collision plane.

Salop[24] has calculated the n- and l-dependent cross sections for the collisions of B^{5+}, C^{6+}, and O^{8+} ions with atomic hydrogen at intermediate collision energies ($v_{rel} = 1$–1.7 a.u.), using the Monte Carlo classical trajectory method. Figures 11 and 12 show the comparisons of the n-dependent cross sections obtained by him with the UDWA results for the case of C^{6+} + H(1s) collision energies of 25 and 75 keV/amu. Figures 13 and 14 present the l-dependent cross sections for the same collision system and for the case of $n = 4$. Salop supposed that the classical energy and momentum of the captured electron which are within 0.5 of the integer n and l correspond to the quantum numbers n and l, respectively. Because of such a rule of correspondence, a little ambiguity is included in the distributions and unphysical transitions into the state of $l > n - 1$ are seen, as shown by shadow marks in Figs. 13 and 14. Considering the situations described above, it can be concluded that the results obtained with both methods show fairly good agreement.

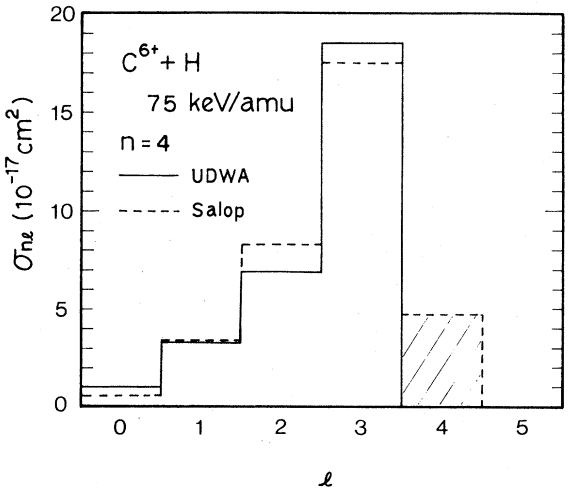

FIG. 14. Same as Fig. 13 for a collision energy of 75 keV/amu.

V. CONCLUDING SUMMARY

We have examined the total cross sections for charge transfer in collisions of H^+, He^{2+}, Li^{3+}, Be^{4+}, B^{5+}, C^{6+}, O^{8+}, Ne^{10+}, Si^{14+}, and Ca^{20+} ions with atomic hydrogen, and have also examined partial cross sections for C^{6+} + H, Ne^{10+} + H, and Se^{14+} + H collision systems. The results show that:

(a) It is useful to scale the energy dependence of the total charge transfer cross section as

$$\sigma(E) = \alpha\tilde{\sigma}(\tilde{E}), \quad E = \beta\tilde{E},$$

with

$$\alpha = Z^{1.07} \text{ and } \beta = Z^{0.464},$$

where $\tilde{\sigma}$ and $\tilde{E}$ are the scaled cross section and impact energy, respectively.

(b) At low impact energies (<10 keV/amu), the distributions of final-state population over n indicate a maximum at $n = n_m$ determined from the effective outer level-crossing point, and the distributions for $n > n_m$ are vanishingly small. With increasing impact energy up to about 100 keV/amu, the distribution becomes broader, while n_m, at which the distributions indicate a maximum, remains almost unchanged. With increasing impact energy greater than 100 keV/amu, the broadness of the distributions and n_m decrease considerably.

(c) At low impact energies, distributions over l for a given n denote larger values at the particular l's due to the effects of the level crossing. At intermediate impact energies, the distributions indicate a maximum at $l = n - 1$ for the higher values of n and indicate a maximum at $l < n - 1$ for lower values of n. At high impact energy (~500 keV/amu), the distributions are completely free from the influence of level crossing, but are strongly affected by momentum-transfer effects. Consequently, the distributions are suppressed at the higher values of l.

(d) Distributions over m for given l and n indicate a maximum at $m=0$ except for the cases of low-energy impacts.

ACKNOWLEDGMENTS

The authors would like to express their thanks to Dr. D. H. Crandall, Dr. F. W. Meyer, Dr. R. A. Phaneuf, Dr. H. J. Kim, Dr. P. Hvelplund, and Dr. P. H. Stelson for providing us with their experimental data prior to publication. Thanks are also due to Miss Kayoko Hirai for her continual assistance in computation and in preparing of this paper.

---

*Visiting fellow for 1978–79, FOM Institute for Atomic and Molecular Physics, Kruislaan 407, Amsterdam, The Netherlands.

[1]H. Ryufuku and T. Watanabe, Phys. Rev. A 18, 2005 (1978).
[2]A. Salop and R. E. Olson (private communication).
[3]R. E. Olson and A. Salop, Phys. Rev. A 16, 531 (1977).
[4]A. Salop and R. E. Olson, Phys. Rev. A 13, 1312 (1976).
[5]C. Bottcher, J. Phys. B 10, L213 (1977).
[6]R. E. Olson and A. Salop, Phys. Rev. A 14, 579 (1976).
[7]A. Salop and R. E. Olson, Phys. Rev. A 16, 1811 (1977).
[8]J. Vaaben and J. S. Briggs, J. Phys. B 10, L521 (1977).
[9]C. Harel and A. Salin, J. Phys. B 10, 3511 (1977).
[10]H. Ryufuku and T. Watanabe, Phys. Rev. A 19, 1538 (1979).
[11]M. B. Shah, T. V. Goffe, and H. B. Gilbody, J. Phys. B 11, L233 (1978).
[12]R. A. Phaneuf, F. W. Meyer, R. H. McKnight, R. E. Olson, and A. Salop, J. Phys. B 10, L425 (1977).
[13]R. A. Phaneuf, F. W. Meyer, and R. H. McKnight, Phys. Rev. A 17, 534 (1978).
[14]H. J. Kim, R. A. Phaneuf, F. W. Meyer, and P. H. Stelson, Phys. Rev. A 17, 854 (1978).
[15]L. D. Gardner, J. E. Bayfield, P. M. Koch, H. J. Kim, and P. H. Stelson, Phys. Rev. A 16, 1415 (1977).
[16]J. E. Bayfield, P. M. Koch, L. D. Gardner, I. A. Sellin, D. J. Pegg, R. S. Peterson, and D. H. Crandall, in Contributed Papers of the Fifth International Conference on Atomic Physics, Berkeley, 1976, edited by R. Marrus, M. H. Prior, and H. A. Shugart (unpublished), p. 126; revised values in L. D. Gardner, Ph.D. dissertation, Yale University, 1978 (unpublished).
[17]F. W. Meyer, R. A. Phaneuf, H. J. Kim, P. Hvelplund, and P. H. Stelson, Phys. Rev. A 19, 515 (1979).
[18]D. H. Crandall, R. A. Phaneuf, and F. W. Meyer, Phys. Rev. A 19, 504 (1979).
[19]K. H. Berkner, W. G. Graham, R. V. Pyle, A. S. Schlachter, J. W. Stearns, and R. E. Olson, J. Phys. B 11, 875 (1978).
[20]K. H. Berkner, W. G. Graham, R. V. Pyle, A. S. Schlachter, and J. W. Stearns, Phys. Lett. A 62, 407 (1977).
[21]J. Hamilton, *The Theory of Elementary Particles* (Clarendon, Oxford, 1959), p. 213.
[22]D. R. Bates, Proc. R. Soc. A 247, 294 (1958).
[23]W. L. Nutt, R. W. McCullough, K. Brady, M. B. Shah, and H. B. Gilbody, J. Phys. B 11, 1457 (1978).
[24]A. Salop, J. Phys. B 12, 919 (1979).